J. Phys. B: At. Mol. Opt. Phys. **23** (1990) 3629-3642. Printed in the UK

Ion–atom excitation at high and intermediate energies

V D Rodríguez and J E Miraglia

Instituto de Astronomía y Física del Espacio†, Casilla de Correos 67, Sucursal 28, 1428 Buenos Aires, Argentina

Received 22 January 1990, in final form 26 June 1990

Abstract. Exact post and prior impulse approximation cross sections are calculated for the excitation process $H^+ + H(1s \to n = 2)$. The results show a large post-prior discrepancy and a huge disagreement with the experiments, even at energies where the simple Born approximation already works. Following a previous work along this line, we show that the theory remarkably improves when the correct asymptotic conditions are observed by including eikonal phases. This new approximation, called the eikonal impulse approximation, presents a negligible prior-post discrepancy at high energies and the prior version produces very good agreement with the experiments. Departure of the total excitation cross section from the quadratic law on the projectile charge (saturation) is discussed and compared with the available data. Scaling laws, alignment factors and s-p coherences are reported and compared with previous results.

1. Introduction

Ion-atom excitation has been the object of a large number of both theoretical and experimental studies in recent years (for a review see the work by Park (1983), more recent experimental studies are the works of Wohrer *et al* (1986) and Reymann *et al* (1988)). From the theoretical point of view, most effort was directed to solving the time-dependent Schrödinger equation for the electron motion, for which a close-coupling procedure is generally performed (see, for example, Jain *et al* 1988 and references therein). However, as the projectile charge (Z_P) increases, a great number of (atomic or molecular) states are required, making the numerical solution hard in the intermediate-energy region. By intermediate-energy region in excitation, we mean the specific energy $E(\text{keV amu}^{-1})$ in the range of approximately $15 < E/Z_P < 200\ \text{keV amu}^{-1}$.

On the other hand, it is for this the intermediate-energy region and for the high-energy region, that some distorted-wave methods have been developed (Franco and Thomas 1971, Theodosiou 1980, Reinhold and Miraglia 1987), and they have been quite successful in explaining the experimental results. Common features of them are their relative simplicity and the standardization of the numerical calculation for any charge Z_P.

† The Instituto de Astronomía y Física del Espacio is affiliated to the Consejo Nacional de Investigaciones Científicas y Técnicas from Argentina.

0953-4075/90/203629+14$03.50

In this context, we have developed the symmetric eikonal (SE) distorted-wave method (Reinhold and Miraglia 1987, Rodríguez and Miraglia 1989a, b) which preserves the Coulomb asymptotic conditions on both the initial and final channels. One point that we have observed is that the SE method provides a good description for optically allowed transitions, but it seems to underestimate the forbidden ones when compared with sophisticated close-coupling calculations and the experiments in the intermediate-energy range. The reason for this failure could be understood if we consider that in optically forbidden transitions second-order processes can be competitive with the direct one, that is a forbidden transition is achieved by two successive allowed ones. As discussed by Inokuti (1971 p 340), this two-step transition can be nearly as efficient as the weak direct (optically forbidden) one at intermediate energies (see also Schöller *et al* 1986). Though in the SE distorted-wave method higher orders are included in some way, they are certainly not fully taken into account. Most of the distorted wavefunctions are simply the product of multiplying the unperturbed ones by a Coulomb distortion representing the dispersion of the electron with the projectile at an average relative velocity equal to the relative projectile-target velocity. So a way to improve them is to look for a better wavefunction that considers the electron velocity distribution around the target nucleus as the impulse wavefunction does (Coleman 1969). In the so-called impulse approximation (IA), the multiple scattering of the electron in the field of the projectile is built up into the corresponding wavefunction. As is usual in heavy ion–atom collisions, the internuclear interaction is switched off (Coleman 1969), so the IA method lacks the appropriate Coulomb condition on the non-distorted channel.

In this work, we introduce the eikonal impulse approximation (EIA) as applied to excitation. As we shall see, this method can be considered as an improvement on the SE one to better account for higher-order terms, or as an improvement on the IA approximation where the unperturbed channel is distorted to account for the Coulomb conditions. In a previous work, electron capture in asymmetric collisions was studied with the present EIA (Gravielle and Miraglia 1988), so we refer the reader to this work for further analysis.

2. Theory

In the present article, we study the excitation of a hydrogen-like atom, composed by a nucleus target 'T' (of charge Z_T) and an electron 'e', by a heavy projectile 'P' (Z_P) impinging with velocity v. Atomic units will be used except where indicated. In short, the coordinate systems are given by $\{\boldsymbol{R}_T, \boldsymbol{r}_T\}$ or $\{\boldsymbol{R}_P, \boldsymbol{r}_P\}$ where $\boldsymbol{r}_T(\boldsymbol{r}_P)$ is the position of the electron referred to the target(projectile) nucleus, $\boldsymbol{R}_T$ is the position of 'P' with respect to the centre of mass of the (T–e) pair and $\boldsymbol{R}_P$ is the position of the centre of mass of the (P–e) pair with respect to 'T'. In all the expressions below, the electron mass is neglected as compared with the target and projectile masses. Throughout the work the internuclear interaction will be dropped and reintroduced through the well known Coulomb phase factor (see, for example, Reinhold and Miraglia 1987), when calculating the differential cross section.

2.1. The exact impulse approximation

A complete review on the impulse approximation and related methods can be found in Coleman (1969), where some results of hydrogen atom excitation by impact of

protons within the post impulse approximation are reported. This approach makes use of the Born and impulse wavefunctions in the final and initial channels, respectively, given by

$$\Psi_f^{\mathrm{B}} = \exp(\mathrm{i}\boldsymbol{K}_f \cdot \boldsymbol{R}_{\mathrm{T}})\phi_f(\boldsymbol{r}_{\mathrm{T}}) \tag{2.1}$$

$$\Psi_i^{\mathrm{I}} = \int \mathrm{d}\boldsymbol{q}\, \tilde{\phi}_i(\boldsymbol{q}) \exp[\mathrm{i}(\mu_{\mathrm{T}}\boldsymbol{K}_i + \boldsymbol{q}) \cdot \boldsymbol{R}_{\mathrm{P}} + \mathrm{i}(\boldsymbol{q} - \boldsymbol{v}) \cdot \boldsymbol{r}_{\mathrm{P}}] D^+(Z_{\mathrm{P}}, \boldsymbol{q} - \boldsymbol{v}; \boldsymbol{r}_{\mathrm{P}}) \tag{2.2}$$

where $\boldsymbol{K}_{i,f}$ are the initial and final momenta, $\phi_{i,f}(\boldsymbol{r}_{\mathrm{T}})$ are the initial and final electronic wavefunctions, the tilde denotes the Fourier transform (normalized to $(2\pi^{-3})\delta_{i,f}$), μ_{T} is the (T-e) reduced mass and

$$D^{\pm}(Z, \boldsymbol{p}; \boldsymbol{r}) = \exp(\pi a/2)\Gamma(1 \mp \mathrm{i}a))_1 F_1(\pm \mathrm{i}a, 1; \pm \mathrm{i}pr - \mathrm{i}\boldsymbol{p} \cdot \boldsymbol{r}) \tag{2.3}$$

with $a = Z/p$. The T matrix then reads $T^{\mathrm{I}+} = \langle \Psi_f^{\mathrm{B}} | W_i^{\mathrm{I}} | \Psi_i^{\mathrm{I}} \rangle = \langle \Psi_f^{\mathrm{B}} | W_f^{\mathrm{B}+} | \Psi_i^{\mathrm{I}} \rangle$, where W_i and W_f are the initial and final perturbations, i.e.

$$(H - E)\Psi_i^{\mathrm{I}} = W_i^{\mathrm{I}}\Psi_i^{\mathrm{I}} \qquad \text{and} \qquad (H - E)\Psi_f^{\mathrm{B}} = W_f^{\mathrm{B}}\Psi_f^{\mathrm{B}}. \tag{2.4}$$

Alternatively, the prior impulse approximation (IA$^-$) makes use of impulse and Born wavefunctions in the final and initial channels, respectively, given by

$$\Psi_f^{\mathrm{I}} = \int \mathrm{d}\boldsymbol{q}\, \tilde{\phi}_f(\boldsymbol{q}) \exp[\mathrm{i}(\boldsymbol{K}_f + \boldsymbol{q}) \cdot \boldsymbol{R}_{\mathrm{P}} + \mathrm{i}(\boldsymbol{q} - \boldsymbol{v}) \cdot \boldsymbol{r}_{\mathrm{P}}] D^-(Z_{\mathrm{P}}, \boldsymbol{q} - \boldsymbol{v}; \boldsymbol{r}_{\mathrm{P}}) \tag{2.5}$$

$$\Psi_i^{\mathrm{B}} = \exp(\mathrm{i}\boldsymbol{K}_f \cdot \boldsymbol{R}_{\mathrm{T}})\phi_i(\boldsymbol{r}_{\mathrm{T}}). \tag{2.6}$$

The T matrix element then reads

$$T^{\mathrm{I}-} = \langle \Psi_f^{\mathrm{I}} | W_i^{\mathrm{B}} | \Psi_i^{\mathrm{B}} \rangle = \langle \Psi_f^{\mathrm{I}} | W_f^{\mathrm{I}+} | \Psi_i^{\mathrm{B}} \rangle.$$

2.2. The eikonal impulse approximation

Since the optically allowed transition takes place at relatively large impact parameters (Rodríguez and Miraglia 1989b), the use of wavefunctions having the proper long distance behaviour (on both channels) would result in an improvement. This is accomplished by including the eikonal wavefunctions instead of the Born ones, given by

$$\Psi_f^{\mathrm{E}} = \Psi_f^{\mathrm{B}} E^-(Z_{\mathrm{P}}, -\boldsymbol{v}; \boldsymbol{r}_{\mathrm{P}}) \tag{2.7}$$

$$\Psi_i^{\mathrm{E}} = \Psi_i^{\mathrm{B}} E^+(Z_{\mathrm{P}}, -\boldsymbol{v}; \boldsymbol{r}_{\mathrm{P}}) \tag{2.8}$$

where

$$E^{\pm}(Z, \boldsymbol{p}; \boldsymbol{r}) = \exp[\mp \mathrm{i}a \ln(pr \mp \boldsymbol{p} \cdot \boldsymbol{r}) \tag{2.9}$$

with $a = Z/p$.

These wavefunctions—like the exact impulse ones—satisfy the correct asymptotic Coulomb conditions and are properly normalized. In this way we have the so-called eikonal impulse approximations in the post and prior versions: $T^{\mathrm{EI}+} = \langle \Psi_f^{\mathrm{E}} | W_i^{\mathrm{I}} | \Psi_i^{\mathrm{I}} \rangle = \langle \Psi_f^{\mathrm{E}} | W_f^{\mathrm{E}+} | \Psi_i^{\mathrm{I}} \rangle$ and $T^{\mathrm{EI}-} = \langle \Psi_f^{\mathrm{I}} | W_i^{\mathrm{E}} | \Psi_i^{\mathrm{E}} \rangle = \langle \Psi_f^{\mathrm{I}} | W_f^{\mathrm{I}+} | \Psi_i^{\mathrm{E}} \rangle$, labelled by EIA$^+$ and EIA$^-$ respectively. The prior version EIA$^-$ reads

$$T^{\mathrm{EI}-} = -\frac{P^2}{2} \int \mathrm{d}\boldsymbol{K}\, \tilde{\phi}_f^*(\boldsymbol{v} - \boldsymbol{K})\tilde{\phi}_i(\boldsymbol{v} - \boldsymbol{K} - \boldsymbol{P})\left(1 + \frac{2\boldsymbol{P} \cdot \boldsymbol{K}}{P^2}\right) G^-(-\boldsymbol{P}; Z_{\mathrm{P}}, -\boldsymbol{K}; Z_{\mathrm{P}}, \boldsymbol{v}) \tag{2.10}$$

where

$$G^{-}(\boldsymbol{Q}; Z_1, \boldsymbol{p}_1; Z_2, \boldsymbol{p}_2) = \int \mathrm{d}\boldsymbol{r} \exp(\mathrm{i}\boldsymbol{Q}\cdot\boldsymbol{r}) D^{-*}(Z_1, \boldsymbol{p}_1; \boldsymbol{r}) E^{+}(Z_2, -\boldsymbol{p}_2; \boldsymbol{r}) \tag{2.11}$$

and $\boldsymbol{P} = \boldsymbol{K}_i - \boldsymbol{K}_f$ is the momentum transfer vector. Closed forms of this integral in terms of hypergeometric functions ${}_2F_1$ are presented in the appendix. The post version EIA$^+$ has a similar integral expression

$$T^{\mathrm{EI}+} = -\frac{P^2}{2} \int \mathrm{d}\boldsymbol{K}\, \tilde{\phi}_f^{*}(\boldsymbol{v}+\boldsymbol{K}+\boldsymbol{P}) \tilde{\phi}_i(\boldsymbol{v}+\boldsymbol{K}) \left(1 - \frac{2\boldsymbol{P}\cdot\boldsymbol{K}}{P^2}\right) G^{+}(-\boldsymbol{P}; Z_{\mathrm{P}}, -\boldsymbol{K}; Z_{\mathrm{P}}, \boldsymbol{v}) \tag{2.12}$$

where

$$G^{+}(\boldsymbol{Q}; Z_1, \boldsymbol{p}_1; Z_2, \boldsymbol{p}_2) = \int \mathrm{d}\boldsymbol{r} \exp(\mathrm{i}\boldsymbol{Q}\cdot\boldsymbol{r}) E^{-*}(Z_2, -\boldsymbol{p}_2; \boldsymbol{r}) D^{+}(Z_1, \boldsymbol{p}_1; \boldsymbol{r})$$

$$= G^{-}(\boldsymbol{Q}; Z_1, -\boldsymbol{p}_1; Z_2, -\boldsymbol{p}_2). \tag{2.13}$$

The symmetric eikonal (SE) approach is obtained by approximating the exact impulse wavefunctions, in either EIA$^+$ or EIA$^-$, by the eikonal ones. The T-matrix element then reads: $T^{\mathrm{SE}} = \langle \Psi_f^{\mathrm{E}} | W_i^{\mathrm{E}} | \Psi_i^{\mathrm{E}} \rangle = \langle \Psi_f^{\mathrm{E}} | W_f^{\mathrm{E}+} | \Psi_i^{\mathrm{E}} \rangle$, and it has closed form for any transition as shown in Reinhold and Miraglia (1987) (further, the first Born approximation is simply given by $T^{\mathrm{B}} = \langle \Psi_f^{\mathrm{B}} | W_{i,f}^{\mathrm{B}} | \Psi_i^{\mathrm{B}} \rangle$). In this way, we can consider the EIA approximation as an improvement on the SE where $\Psi_{i(f)}^{\mathrm{E}}$ is replaced by $\Psi_{i(f)}^{\mathrm{I}}$ to account for the multiple scattering of the electron in the field of the projectile, or an improvement on the exact impulse approximation where $\Psi_{i(f)}^{\mathrm{B}}$ is replaced by $\Psi_{i(f)}^{\mathrm{E}}$ to account for the proper Coulomb conditions.

2.3. Validity range and the post–prior discrepancy

At this point we would like to examine the validity and the post–prior discrepancy of the present eikonal impulse approximation, in terms of the region of projectile charges and impact velocities. As mentioned before, the eikonal wavefunction provides the Coulomb asymptotic condition, while the exact impulse one should be considered as an approximation to the exact scattering wavefunction. In this way, the validity range of the eikonal impulse approximation is related to the corresponding one of the impulse wavefunction, though the range can be actually wider, owing to the improvement of the eikonal wavefunction over the wavefunction having only the correct asymptotic condition.

It is well known that by using exact scattering wavefunctions, the post and prior results should not differ from each other. This is not the present case, since the impulse wavefunction is designed to represent the exact one in the high-energy region, where the impulse hypothesis is valid (Coleman 1969). The high-energy region can be characterized by considering the perturbative parameter Z_{P}/v less than unity. Thus, the validity of the eikonal impulse approximation, and therefore a negligible post–prior discrepancy, would be expected for, say $Z_{\mathrm{P}}/v < 0.5$ ($E > 100$ keV for protons on hydrogen). However, the question is which version to choose, if it is desired to extend the region of validity to the intermediate-energy one. In the next two paragraphs, we put forward an *a priori* criterion based on the non-equivalence of both the initial and final impulse wavefunctions, with respect to the impulse hypothesis.

The impulse wavefunctions Ψ_i^I and Ψ_f^I are approximations to the exact ones in the initial and final channels, respectively. We know that for the excitation process, the mean velocity of the electron in the final excited state (v_f) is smaller than that of the initial one (v_i). Since $v_f/v < v_i/v$, the final impulse wavefunction is then in a better condition than the initial one to describe the collision process, in accordance with the impulse hypothesis, i.e. the collision time should be short compared with typical orbital times. So this is an argument in favour of the use of the final impulse wavefunction, which leads us to the prior version EIA$^-$.

A further support to the choice of the prior version arises from a time-dependent analysis. As Ψ_i^I and Ψ_f^I are approximations of the initial and final channels; or, in other words, for positive and negative collision times we should ask whether the collision mainly takes place at positive or negative times. The answer can be drawn from figure 1 of Ast *et al* (1988), or figure 4 of Grün (1987), where the excitation probabilities as a function of time are plotted. There, it is clearly seen that the population of 2s and 2p excited states takes place mainly for positive times, and further, both states are still coupled at very large internuclear distances (Stark mixed). For instance, Grün (1987) found that for Li^{3+} impact on hydrogen the excitation probability is negligible for negative times, while it increases for positive times, peaking at $z = vt \sim +5$. Therefore, it is clear that an as-good-as-possible description of the final channel is needed, and so we should use Ψ_f^I which leads us to the prior version EIA$^-$ again.

The same arguments can also be used to justify the choice of the prior version of other distorted-wave methods having prior–post discrepancies, such as the VPS approximation as presented by Theodosiou (1980) and Sinha *et al* (1987). Though Theodosiou (1980) made a peaking approximation in his calculations, the exact evaluation of Sinha *et al* (1987), shows that the exact VPS presents a post–prior discrepancy and that the prior form gives fair agreement with experiments for electron–atom excitation (these authors called the post form what Coleman (1969) and ourselves call the prior one).

3. Results and discussion

We have computed excitation cross sections in the prior and post forms of the eikonal impulse approximation. The task requires calculation of the three-dimensional integrals (2.10) and (2.12), which have been numerically performed. As usual, another numerical integral on the angular distributions is required to achieve a total cross section.

We have also computed cross sections in the impulse approximation which can be readily obtained by setting $Z_2 = 0$ instead of $Z_2 = Z_P$ in equation (2.10) (impulse prior), or in equation (2.12) (impulse post). So calculations of both the impulse and eikonal impulse T matrices have been made with the same computer code. In order to test the numerical integrations we have compared the present IA$^+$ cross sections with those listed by Coleman (1968) for 2s hydrogen excitation by impact of protons. The results were found to be in quite good agreement (within 1%).

3.1. Total cross sections

Cross sections (σ) for the process:

$$H^+ + H(1s) \rightarrow H^+ + H(n = 2) \tag{3.1}$$

are shown in figure 1. Calculations in the eikonal impulse approximation, labelled by

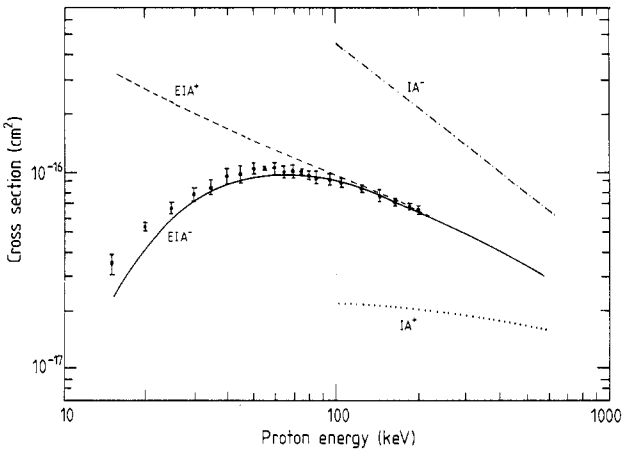

Figure 1. Excitation cross sections of hydrogen to $n = 2$ by impact of protons. Experiments of Park *et al* (1976). Theory: IA$^+$ and IA$^-$ post and prior exact impulse approximations; EIA$^+$ and EIA$^-$ post and prior eikonal impulse approximations as indicated in the text.

EIA$^+$ and EIA$^-$ (post and prior versions respectively) show a good agreement with the experimental results (Park *et al* 1976) for energies larger than 100 keV, i.e. $Z_P/v < 0.5$. For these energies the post-prior discrepancy in the eikonal impulse approximation is negligible. On the contrary, in the impulse approximation the post-prior discrepancy remains considerable up to energies as large as 500 keV. The impulse post and impulse prior results (labelled by IA$^+$ and IA$^-$ respectively), show a large disagreement with the data. It should be noted that the experimental data have been normalized at 200 keV to the Born approximation (Park *et al* 1976). Both versions approach the first Born approximation at *very* high impact energies.

In the intermediate-energy range, from the comparison with the experiments, we can affirm that the prior version EIA$^-$ exhibits a considerably better performance than the post one, in agreement with our theoretical considerations of section 2.3. Hereinafter, our analysis is restricted to the prior versions EIA$^-$ and IA$^-$.

Individual excitation to 2s and 2p of hydrogen by impact of protons is shown in figures 2(*a*) and 2(*b*). The method gives a good description of the extended data (Park 1983) up to energies as small as 25 keV, quite reasonable for a distorted-wave method. In particular, the 2s excitation cross section is known to be much more sensitive to the choice of the approximation than is the 2p excitation; only the most accurate calculations give good results for this transition, as indicated by Park (1983). On the other hand, the total 2p excitation has been quite well described by other distorted-wave methods, such as the Glauber theory (Franco and Thomas 1971) and the symmetric eikonal (Reinhold and Miraglia 1987).

Figure 2 also compares EIA$^-$ with the IA$^-$ and SE methods, from where we can extract valuable physical information in the intermediate-energy range. For 2p excitation, SE works well while IA$^-$ does not. The explanation of this feature is simple: optically allowed transitions take place at relatively large distances in a single step, so just the Coulomb conditions—included in the SE method—are enough to explain the data, while higher orders included in the IA$^-$ are ineffective. On the contrary, for 2s excitation the roles change, that is: the forbidden transitions take place at relatively smaller distances (than permitted ones) via two-step processes. In this way the higher

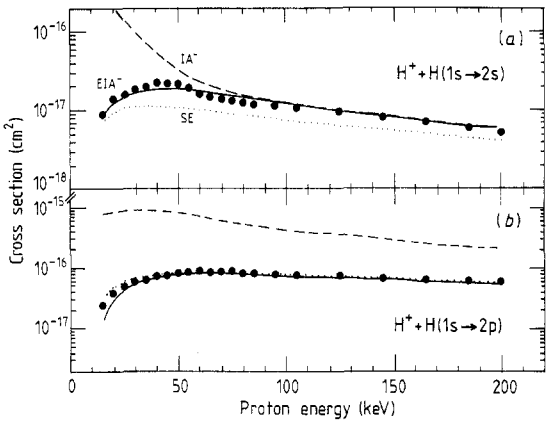

Figure 2. (*a*) Excitation to 2s of hydrogen by impact of protons as a function of the impact energy. Full circles: extended data from figure 10 of Park (1983). Theory: IA$^-$ and EIA$^-$, prior versions of the exact impulse and eikonal impulse approximations; SE, symmetric eikonal method. (*b*) Similar to (*a*) for excitation to 2p.

orders included in the IA$^-$ describe such double processes, while the proper long-distance behaviour of the SE wavefunctions is ineffective. The EIA$^-$ has the best of both worlds, that is, the higher order included in Ψ_f^I and the correct Coulomb conditions on both channels.

In table 1 we compare the detailed EIA$^-$ cross sections for excitation to the 2s and 2p states with other theoretical results, such as: the ones obtained by solution of the coupled-state equations with two basis sets containing up to seven s, five p, and three d state orbitals (Bransden and Noble 1978, Bransden *et al* 1979), Shakeshaft's coupled-equations results (Shakeshaft 1978) with 35 scaled hydrogenic wavefunctions on both centres, and those obtained by application of the Schwinger variational principle of Brendlé *et al* (1985). At the energy of 50 keV, the results of Bransden *et al* (1979) are

Table 1. Total cross sections (in units of 10^{-17} cm^2) of atomic hydrogen excitation to the $n=2$ level by proton impact at 50, 105 and 145 keV in the laboratory. BDN, S, SCHW: theoretical results of Bransden *et al* (1979), Shakeshaft (1978), and Brendlé *et al* (1985), respectively; EIA$^-$: present calculations; EXP: experimental data of Park *et al* (1976).

	BDN	S	SCHW	EIA$^-$	EXP
			$E_{lab}=50$ keV		
1s→2s	2.69	1.79	1.30	1.88	
1s→2p	9.23	6.88	7.90	7.74	
Total	11.92	8.67	9.20	9.62	10.53 ± 0.64
			$E_{lab}=105$ keV		
1s→2s	1.12		0.76	1.16	
1s→2p	8.20		7.79	7.40	
Total	9.32	8.4	8.54	8.56	8.88 ± 0.29
			$E_{lab}=145$ keV		
1s→2s	0.77	0.80		0.85	
1s→2p	7.09	6.53		6.72	
Total	7.86	7.33		7.57	7.75 ± 0.58

larger than the others; this could be understood if we consider that below this energy, the charge transfer becomes important, so that the cross sections for direct excitation are overestimated by a single-centre expansion method. The agreement of our EIA$^-$ total cross sections with the Shakeshaft's results and with the Schwinger variational calculations is reasonably good at energies of 50 and 105 keV. At the higher energy of 145 keV, both kinds of coupled-state calculations are in good agreement with the present EIA$^-$ results.

3.2. Differential cross sections

Angular distributions calculated with (full curves) and without (broken curves) internuclear interaction (the internuclear interaction was taken in the eikonal approximation, see for example Reinhold and Miraglia (1987), equations (14) and (15)) are shown in figure 3 for reaction (3.1). In general, our EIA$^-$ results follow closely the experiments (Park *et al* 1980) as the other theoretical calculations displayed in the figure also do. At 50 keV, the theory seems to underestimate the data at intermediate angles, in the same way that Shakeshaft's calculations do. On the other hand, the results of Brendlé

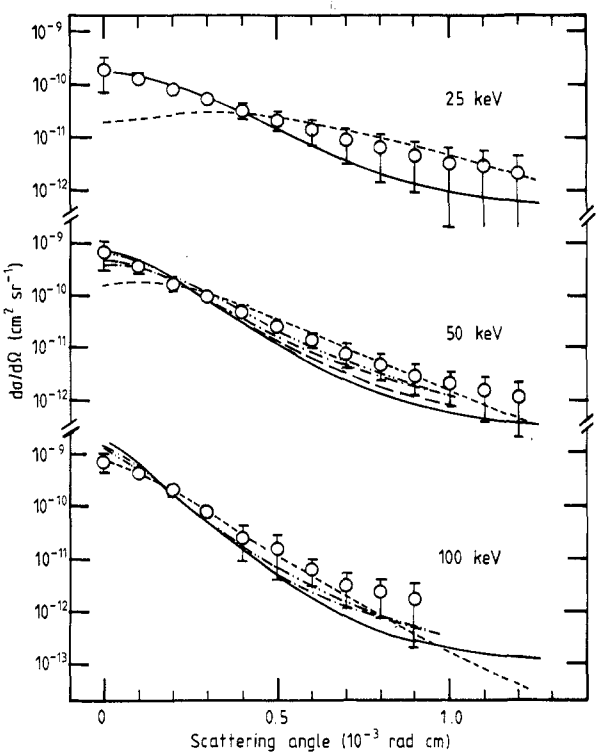

Figure 3. Differential cross section for excitation to $n = 2$ of hydrogen by impact of protons as a function of the centre-of-mass scattering angle at different energies. Experiments of Park *et al* (1980). Theory: full and short dashed broken curves, the present prior eikonal impulse approximation with and without internuclear interaction, respectively; double dotted chain curve, results of Bransden and Noble (1978); long dashed broken curve, Shakeshaft's results (taken from Park 1983); chain curve, Schwinger variational method of Brendlé *et al* (1985). The results of this last theory shown in the figure at 100 keV, were actually calculated at 105 keV (Brendlé *et al* 1985).

et al (1985) accomplished through the use of the Schwinger variational principle and those of Bransden and Noble (1978), who employed coupled equations, are in better agreement at intermediate angles, though the former seems to be small at small scattering angles. At 100 keV, our theoretical results overestimate the experimental data in the forward direction, but this is a general tendency of all the theories shown in the figure (see also figure 9 of Park 1983).

3.3. Dependence on the projectile charge

Our main concern is the behaviour of the excitation cross section for large projectile charges. In our group, we have studied these phenomena in the symmetric eikonal (Reinhold and Miraglia 1987, Rodríguez and Miraglia 1989a, b, c) and classical trajectory Monte Carlo (Reinhold *et al* 1987) approximations. More precisely, we have explored the possibility of saturation; i.e. the cross section would tend to a constant value as Z_P tends to infinity, as proposed by Brendlé *et al* (1985) by using the Schwinger variational principle. The excitations $1s^2 \rightarrow 1s2p$ and $1s^2 \rightarrow 1s3p$ of Fe^{24+} by impact of bare ions (Z_P charge) were calculated with the present model, and results are shown in figure 4. Two points should be taken into consideration when comparing with the experiments (Wohrer *et al* 1986). First, in the experiments neutral atoms instead of bare projectiles were used. Since the radius of Fe^{24+} is very small, the nuclear charge approximation can be a good description for light atoms. However, for krypton atoms, the nuclear charge is totally shielded by the K shell and partially by the L one (appendix 2 of Reinhold and Miraglia 1987), so the Kr atom behaves as a charge smaller than 34. Second, experiments were corrected (full circles) by cascade and double processes (Wohrer *et al* 1986), except for the Kr atom. It is just in this case that substantial corrections are expected.

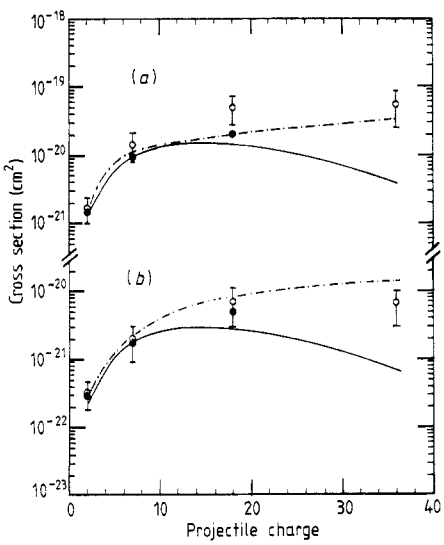

Figure 4. (*a*) $1s \rightarrow 2p$ excitation cross section per electron of 400 MeV Fe^{24+} ions in collisions with He, N, Ar and Kr atoms. Open circles (uncorrected) and full circles (corrected by cascade and double processes) experiments of Wohrer *et al* (1986). Theory: full curve, the present prior eikonal impulse approximation; chain curve, Schwinger variational method (Gayet and Bouamoud 1989). (*b*) Similar to (*a*) for excitation $1s \rightarrow 3p$.

However, despite such considerations it is clearly appreciated in figures 4(*a*) and 4(*b*), that there is a disagreement of the EIA$^-$ results with the experimental data for the larger nuclear charges. This failure in the theory can be anticipated if one examines the region of the projectile charges Z_P and velocities v where the EIA$^-$ would be expected to be valid, at least where $Z_P/v < 1$. In fact, as the velocity of the 400 MeV Fe^{24+} ion is $v = 16.9$ (au), the inequality above implies that $Z_P < 17$; in this way, beyond $Z_P = 17$ the theory is out of its validity range, precisely where the theoretical results begin to depart from the experimental data.

In the same figures, the new theoretical results of Gayet and Bouamoud (1989) obtained by application of the Schwinger variational principle are also displayed. The agreement of this theory with the experimental data is good, even for larger nuclear charges.

3.4. Scaling laws

Fritsch and Schartner (1987) have recently studied the scaling properties of 2p excitations in collision between one-electron ground-state targets and multiply charged ions. Following a parametrization introduced by Janev and Presnyakov (1980, hereafter referred to as JP), these authors have found that σ/Z_P lies approximately on a universal curve when plotted in terms of the reduced energy $E/Z_P = 25v^2/Z_P$ in the so-called intermediate energy region, say between 15 and 100 keV amu^{-1}. In a recent article (Rodríguez and Miraglia 1989a), we have studied in detail the JP parametrization and other scaling laws with the SE theoretical model. Here, we present an equivalent study for the EIA$^-$ theoretical method. Figure 5 shows 2p and 2s excitation cross sections of hydrogen by impact of multiply charged ions in terms of the JP parameters. We can summarize the performance as follows.

(i) For 2p excitation (optically allowed transitions), the results follow the JP scaling, and further, they are quite close to the corresponding SE results (see figure 2 of Rodríguez and Miraglia 1989a).

(ii) For 2s excitation (optically forbidden) the results follow the JP scaling, for say $Z_P > 4$ (we note that those obtained with the SE approximation rigorously follow the

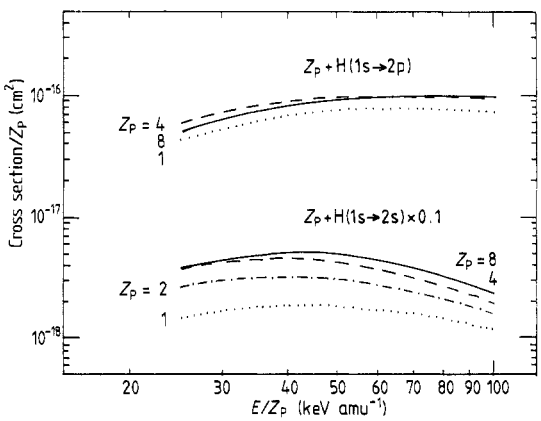

Figure 5. Excitation cross sections of hydrogen to 2p and 2s states by impact of multicharged ions calculated with the EIA$^-$ theoretical method. The curves are scaled in terms of the parameters of Janev and Presnyakov (1980), i.e. σ/Z_P versus E/Z_P, where E is the specific impact energy (keV amu^{-1}).

JP scaling). Further, the EIA$^-$ cross sections displayed in figure 5 are larger than those of the SE (see again figure 2 of Rodríguez and Miraglia 1989a).

3.5. Alignment factor

A very sensitive parameter related to 2p excitation can be used to test the theory more deeply, it is the so-called alignment factor A_{20}, defined as

$$A_{20}=\frac{\sigma_{2p_1}-\sigma_{2p_0}}{2\sigma_{2p_1}+\sigma_{2p_0}}. \tag{3.2}$$

For instance, the Glauber theory gives a constant value $A_{20}=0.5$ (Tai *et al* 1970) in contrast to the first Born approximation, except in the very high energy limit. The alignment factor can be related to the experimental degree of linear polarization P measured by Kauppila *et al* (1970), through $A_{20}=6P/(P-3)$ where $P=(I_{\parallel}-I_{\perp})/(I_{\parallel}+I_{\perp})$ (Hippler *et al* 1988), as plotted in figure 6 for the proton hydrogen case. Although the error bars of the experiments are very large to draw a definite conclusion, the EIA$^-$ would seem to follow the experiments. For energies larger than about 200 keV, the theoretical results tend to the first Born approximation ones. Results of A_{20} for different projectile charges are also plotted in figure 6 in the intermediate energy range as a function of the reduced energy E/Z_P. It is very interesting to remark that, even though 2p excitation cross sections follow quite well the JP scaling, A_{20} does not. We find quantitative disagreement between the present A_{20} calculations and those obtained with SE for $Z_P>2$.

3.6. s-p coherence

Other sensitive parameters related to $n=2$ manifold excitation are the real and imaginary parts of the s-p coherence, $\langle D_z\rangle$ and $\langle \boldsymbol{L}\times\boldsymbol{A}\rangle_z$ respectively, as defined by equations (12*a*) and (12*b*) of Jain *et al* (1987).

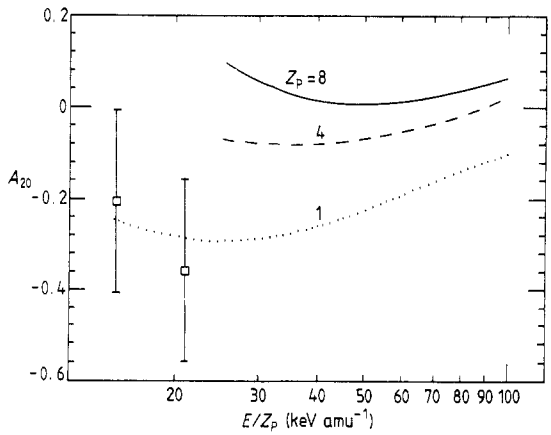

Figure 6. Alignment factor A_{20} as a function of E/Z_P for different projectile charges. Full circles denote A_{20} related to experimental polarization of Kauppila *et al* (1979) through equation (5) of Hippler *et al* (1988). All the curves are theoretical results calculated with the EIA$^-$ method.

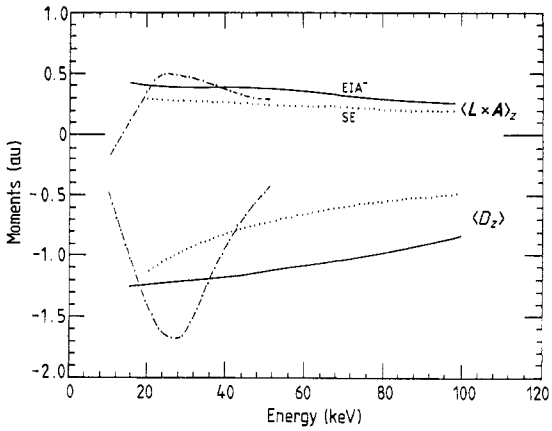

Figure 7. s-p coherences or moments $\langle \boldsymbol{L} \times \boldsymbol{A} \rangle_z$ and $\langle D_z \rangle$ as a function of the impact energy. Full and dotted curves are the theoretical results calculated with the EIA$^-$ and SE theoretical methods, respectively. Chain curves are the results of Jain *et al* (1981) obtained with the two-centre atomic close-coupling calculation.

In figure 7, we plot the moments $\langle \boldsymbol{L} \times \boldsymbol{A} \rangle_z$ and $\langle D_z \rangle$ for proton–hydrogen excitation, and they are compared with the theoretical results of Jain *et al* (1987) calculated with the two-centre atomic centre expansion method. Although there is not a good quantitative agreement with the close-coupling calculations, the EIA$^-$ predicts the same sign, and similar magnitude and slope. In the same figure we show results obtained with the SE theoretical method. From the comparison, we can say that although the SE results have the same qualitative behaviour, the moment $\langle D_z \rangle$ seems to be more sensitive to the theoretical approach.

4. Concluding remarks

In this work we have calculated the exact post and prior impulse approximations and compared the results with experimental data, so that a clear assessment of the theories is made. Besides previous results by Coleman (1968), this is the first time, as far as we know, that this kind of results are presented. We conclude that neither post nor prior theories are capable of accounting for the experimental data in the intermediate- to high-energy range.

Within the distorted-wave formalism a considerable improvement can be accomplished through the replacement of the unperturbed wavefunctions by eikonal ones, in this way we have introduced the eikonal impulse approximation EIA in the context of ion–atom excitation. An *a priori* criterion has been stated implying the prior eikonal impulse approximation EIA$^-$ as the more reliable version for the intermediate-energy range.

This theory uses the exact impulse and eikonal wavefunctions on the final and initial channels, respectively. Both wavefunctions have proper normalizations and asymptotic conditions. Good agreement with the experiments is found, and a detailed study in terms of the projectile charge is presented. Our main conclusions are twofold. First, the correct treatment of the asymptotic conditions on both channels is necessary to get a good description of excitation as other studies revealed in the context of charge

exchange (Gravielle and Miraglia 1988, Belkić *et al* 1987). Second, the multiple scattering built up into the impulse wavefunction is required to get a good description of forbidden excitations in the intermediate-energy range.

A comparison between the EIA$^-$ and simpler theories, such as the SE, deserves a short comment. To calculate the T-matrix elements, the former involves numerical three-dimensional integrations, while the latter has closed forms. However, a success of the EIA$^-$ is a precise prediction of the data *within* its range of validity for *both* optically allowed and forbidden transitions. From our experience of multiply charged ions on helium the SE model works very well in the intermediate-energy region only for optically allowed transitions. For comparison of SE model results with experiments of Reymann *et al* (1988) for optically allowed excitation of multicharged ions on helium, see Rodríguez and Miraglia (1989c). For forbidden excitation, results will be published elsewhere. We plan to apply the present EIA$^-$ approach to treat helium excitation by impact of multicharged ions, for which measurements of both kinds of transitions are available (Reymann *et al* 1988).

Appendix 1. Calculation of the integral of equation (2.11)

As a first step, we look for a related integral:

$$J(\boldsymbol{Q}; Z_1, \boldsymbol{p}_1; Z_2, \boldsymbol{p}_2) = \int \mathrm{d}\boldsymbol{r} \exp(\mathrm{i}\boldsymbol{Q}\cdot\boldsymbol{r}) D^{-*}(Z_1, \boldsymbol{p}_1; \boldsymbol{r}) D^{+}(Z_2, -\boldsymbol{p}_2; \boldsymbol{r}) \tag{A.1}$$

which can be obtained from the Nordsiek (1954) one:

$$\begin{aligned} N(z, \boldsymbol{Q}; Z_1, \boldsymbol{p}_1; Z_2, \boldsymbol{p}_2) &= \int \mathrm{d}\boldsymbol{r} \exp(-zr + \mathrm{i}\boldsymbol{Q}\cdot\boldsymbol{r}) \frac{1}{r} {}_1F_1(\mathrm{i}a_1, 1, \mathrm{i}p_1 r + \mathrm{i}\boldsymbol{p}_1\cdot\boldsymbol{r}) \\ &\quad \times {}_1F_1(\mathrm{i}a_2, 1, \mathrm{i}p_2 r + \mathrm{i}\boldsymbol{p}_2\cdot\boldsymbol{r}) \end{aligned} \tag{A.2}$$

with a parametric derivation, that is:

$$J(\boldsymbol{Q}; Z_1, \boldsymbol{p}_1; Z_2, \boldsymbol{p}_2) = C_f(a_1) C_f(a_2) \lim_{z\to 0^+} \frac{\partial}{\partial z} N(z, \boldsymbol{Q}; Z_1, \boldsymbol{p}_1; Z_2, \boldsymbol{p}_2) \tag{A.3}$$

where $C_f(a) = \exp(\pi a/2)\Gamma(1-\mathrm{i}a)$ and $a_j = Z_j/p_j, j = 1, 2$. Finally the connection of the J integral with the integral of equation (2.11) is straightforward by considering:

$$\begin{aligned} E^+(Z_2, \boldsymbol{p}_2; \boldsymbol{r}) &= \exp[-\mathrm{i}(Z_2/p_2)\ln(p_2 r - \boldsymbol{p}_2\cdot\boldsymbol{r})] \\ &= \lim_{\eta\to\infty} C^+ D^+(Z_2, \boldsymbol{p}_2; \eta\boldsymbol{r}) \\ &= \lim_{\eta\to\infty} C^+ D^+(\eta Z_2, \eta\boldsymbol{p}_2; \boldsymbol{r}) \end{aligned} \tag{A.4}$$

where the phase $C^+ = \exp[+\mathrm{i}(Z_2/p_2)\ln(\eta)]$, together to all the dependence on η are simplified in the final result. After some algebra we found:

$$\begin{aligned} G^-(\boldsymbol{Q}; Z_1, \boldsymbol{p}_1; Z_2, \boldsymbol{p}_2) &= C_f(a_1) C_f(a_2) \lim_{z\to 0^+} \frac{8\pi}{D^2} A_1^{-\mathrm{i}a_1} U_2^{-\mathrm{i}a_2} \left[F\left(z + \mathrm{i}a_1 \frac{B_1}{A_1} + \mathrm{i}a_2 \frac{B_2}{U_2} \right) \right. \\ &\quad \left. - \frac{a_1 a_2}{A_1 U_2} F^+\left(U_3 \frac{B_2}{U_2} + (U_3 - U_2)\frac{B_1}{A_1} - B_3 \right) \right] \end{aligned} \tag{A.5}$$

where

$$U_{1,2}=2(\boldsymbol{p}_{1,2}\cdot\boldsymbol{Q}-\mathrm{i}zp_{1,2})/D \qquad U_3=2(p_1p_2-\boldsymbol{p}_1\cdot\boldsymbol{p}_2)/D \qquad D=Q^2+z^2$$

$$A_j=1+U_j \qquad j=1,2,3 \qquad B_{1,2}=-\mathrm{i}p_{1,2}-zU_{1,2} \qquad B_3=-zU_3$$

$$F={}_2F_1(\mathrm{i}a_1,\mathrm{i}a_2,1;X) \qquad F^+={}_2F_1(1+\mathrm{i}a_1,1+\mathrm{i}a_2,2;X)$$

$$X=(U_1U_2+U_3)/(A_1U_2).$$

In the calculations the limit $z\to 0^+$ has been properly taken into account. Analytical continuations of the hypergeometric functions were made when required.

References

Ast H, Ludde H J and Dreizler R M 1988 *J. Phys. B: At. Mol. Opt. Phys.* **21** 4143

Belkić Dz, Saini S and Taylor H S 1987 *Phys. Rev.* A **36** 1601

Bransden B H, Dewangan D P and Noble C J 1979 *J. Phys. B: At. Mol. Phys.* **12** 3563

Bransden B H and Noble C J 1978 *Phys. Lett.* **70A** 404

Brendlé B, Gayet R, Rozet J P and Wohrer K 1985 *Phys. Rev. Lett.* **54** 2007

Coleman J P 1968 *J. Phys. B: At. Mol. Phys.* **1** 567

—— 1969 *Case Studies in Atomic Collision Theory* vol 1, ed E W McDaniel and M R C McDowell (Amsterdam: North-Holland) p 149

Franco V and Thomas B K 1971 *Phys. Rev.* A **4** 945

Fritsch W and Schartner K H 1987 *Phys. Lett.* **126A** 17

Gayet R and Bouamoud M 1989 *Nucl. Instrum. Methods* B **42** 515

Gravielle M S and Miraglia J E 1988 *Phys. Rev.* A **38** 504

Grün N 1987 *Proc. 15th Int. Conf. on the Physics of Electronic and Atomic Collisions (Brighton)* ed H B Gilbody *et al* (Amsterdam: North-Holland) Invited papers p 345

Hippler R, Madehein H, Harbich W, Kleinpoppen H and Lutz H O 1988 *Phys. Rev.* A **38** 1662

Inokuti M 1971 *Rev. Mod. Phys.* **43** 340

Jain A, Lin C D and Fritsch W 1987 *Phys. Rev.* A **36** 2041

—— 1988 *J. Phys. B: At. Mol. Opt. Phys.* **21** 1545

Janev R K and Presnyakov L P 1980 *J. Phys. B: At. Mol. Phys.* **13** 4233

Kauppila W E, Teubner P J O, Fite W L and Girnius R J 1970 *Phys. Rev.* A **2** 1759

Nordsiek A 1954 *Phys. Rev.* **93** 785

Park J T 1983 *Adv. At. Mol. Phys.* **19** 67

Park J T, Aldag J E, George J M and Peacher J L 1976 *Phys. Rev.* A **14** 608

Park J T, Aldag J E, Peacher J L and George J M 1980 *Phys. Rev.* A **21** 751

Reinhold C O and Miraglia J E 1987 *J. Phys. B: At. Mol. Phys.* **20** 1069

Reinhold C O, Falcon C A and Miraglia J E 1987 *J. Phys. B: At. Mol. Phys.* **20** 3737

Reymann K, Schartner K H, Sommer B and Trabert E 1988 *Phys. Rev.* A **38** 2290

Rodríguez V D and Miraglia J E 1989a *Phys. Rev.* A **39** 6594

—— 1989b *Phys. Lett.* **137A** 123

—— 1989c *Proc. 16th Int. Conf. on the Physics of Electronic and Atomic Collisions (New York)* (Amsterdam: North-Holland) Abstracts p 490

Shakeshaft R 1978 *Phys. Rev.* A **18** 1930

Schöller O, Briggs J S and Dreizler D M 1986 *J. Phys. B: At. Mol. Phys.* **19** 2505

Sinha C, Roy K and Sil N C 1987 *J. Phys. B: At. Mol. Phys.* **20** 2545

Tai H, Bassel R H and Gerjuoy E 1970 *Phys. Rev.* A **1** 1819

Theodosiou C E 1980 *Phys. Rev.* A **22** 2556

Wohrer K, Chetioui A, Rozet J P, Jolly A, Fernandez F, Stephan C, Brendlé B and Gayet R 1986 *J. Phys. B: At. Mol. Phys.* **19** 1997